LoRaWAN vs. IEEE 802.11p: A Reproducible Comparative framework under Realistic V2I Conditions

David Lutala[a] and Ismail Bennis[b]

[a]Vietnam National University, Hanoi, Vietnam
[b]IRIMAS UR 7499, University of Haute Alsace, Mulhouse, France
Email: {davidlutala0@gmail.com, ismail.bennis}@uha.fr

***Abstract*—Today, the main communication technologies driving Intelligent Transportation Systems (ITS) are IEEE 802.11p and 5G NR-V2X, both designed for high-throughput, low-latency vehicular applications. However, these technologies face coverage and cost limitations, particularly in rural and low-infrastructure environments. In contrast, Low Power Wide Area Networks (LPWAN)—and especially LoRaWAN—offer long-range, low-energy connectivity but remain insufficiently explored in dynamic vehicular contexts. This paper presents a rigorous and reproducible comparative study of LoRaWAN and IEEE 802.11p under realistic Vehicle-to-Infrastructure (V2I) conditions. Using a unified NS-3 framework coupled with synchronized SUMO mobility traces and a calibrated HybridBuildings propagation model, both technologies are evaluated within identical spatial, temporal, and physical contexts. Results show that LoRaWAN maintains a high packet delivery ratio (up to 85% within a range of 4 km) and strong resilience under mobility (up to 72 km/h), making it suitable for delay-tolerant periodic V2I communications. Conversely, IEEE 802.11p achieves sub-10 ms latency and higher throughput but experiences sharp reliability degradation beyond 800 m under non-line-of-sight conditions. The proposed framework and the open simulation dataset establish a reproducible foundation for future research on adaptive radio access and cross-technology optimization in vehicular networks.**

***Index Terms*—V2X communication, LoRaWAN, VANET, IEEE 802.11p, Internet of Vehicles, NS-3, propagation modeling.**

I. Introduction

The growing demand for reliable, low-latency, and energy-efficient connectivity in Intelligent Transportation Systems (ITS) has fueled intensive research on vehicular communication technologies, collectively known as Vehicle-to-Everything (V2X). Traditional solutions such as IEEE 802.11p (DSRC) and 5G NR-V2X [1] have become the cornerstone of high-throughput and low-delay vehicular applications. However, these technologies remain constrained by their limited coverage, high infrastructure costs, and scalability challenges in suburban and rural environments.

Conversely, Low Power Wide Area Networks (LPWAN), particularly LoRaWAN, offer long-range connectivity and ultra-low energy consumption. Yet, their applicability in highly dynamic vehicular environments remains largely unexplored. Most existing LoRaWAN studies have focused on static deployments, emphasizing scalability, interference management, and the Adaptive Data Rate (ADR) mechanism [2]–[5]. These works, typically limited to small-scale experiments or simplified simulations, neglect real vehicular mobility and the complexity of urban radio propagation channels.

While IEEE 802.11p has been extensively analyzed in the context of Vehicular Ad Hoc Networks (VANETs), to the best of our knowledge, no prior study has conducted a direct and controlled comparison with LoRaWAN under identical experimental conditions. The absence of a reproducible simulation framework integrating both technologies leaves open fundamental questions about their respective trade-offs in terms of range, reliability, and latency [6], [7]. Existing LoRaWAN implementations in NS-3 [8] rarely incorporate realistic mobility traces or complex propagation environments, limiting the generalizability of their findings.

In this context, the present work proposes a comprehensive comparative evaluation of LoRaWAN and IEEE 802.11p performance in a realistic V2I scenario involving several hundred mobile vehicles. We develop a reproducible simulation framework in NS-3 [8] integrating a LoRaWAN module [5] and IEEE 802.11p, coupled with SUMO [9] mobility traces derived from OpenStreetMap (OSM) and an *HybridBuildings* propagation model accounting for buildings, tunnels, and obstruction losses. This setup enables fine-grained instrumentation of key metrics, including Packet Delivery Ratio (PDR), latency and Time-on-Air (ToA) establishing a rigorous foundation for large-scale VANET performance analysis.

Moreover, we provide an open and structured dataset generated from our simulation campaigns, containing detailed PHY/MAC performance logs for both LoRaWAN and IEEE 802.11p. This dataset is designed for reusability by the research community, particularly for applications involving machine learning, adaptive optimization, and predictive modeling in vehicular networks.

The main contributions of this work can be summarized as follows:

- We implement a complete LoRaWAN simulation framework in NS-3 [8], integrating SUMO [9]-based mobility and a realistic urban propagation model,

- We establish a comparative evaluation of LoRaWAN and IEEE 802.11p under identical V2I conditions, highlighting trade-offs in reliability (PDR), latency, and communication range,
- We made an in-depth parametric analysis of LoRaWAN behavior under mobility,
- We provide an open, structured dataset to support future research on intelligent vehicular communications and AI-driven optimization approaches.

The remainder of this paper is organized as follows: Section II reviews the related work on LoRaWAN and vehicular communications. Section III presents the simulation architecture and the methodology. Section IV details the obtained results with discussion, and Section V concludes the paper with future research direction.

II. Related Work

Vehicular communication technologies have been extensively investigated in the context of VANETs, with significant focus on routing protocols, mobility models, and MAC-layer technologies such as IEEE 802.11p (DSRC). These studies have helped characterize the performance of vehicular networks in highly dynamic environments; however, most have relied on single-technology setups, without integrating low-power, long-range alternatives such as LoRaWAN. In what follows, we provide an overview of existing studies on vehicular communication technologies, emphasizing both LoRaWAN and IEEE 802.11p research in vehicular contexts.

A. IEEE 802.11p and VANET Studies

IEEE 802.11p is the most extensively studied technology in VANETs. In [10], the authors compared five routing protocols—AODV, DSDV, OLSR, GPSR, and GPCR—using NS-3 over an urban map of Oujda, Morocco. However, their study lacked temporal analysis and evaluation of RSU (Road Side Units) coverage. Similarly, the authors in [11] examined OLSR and AODV in intersection-based scenarios, but did not incorporate realistic propagation models or track metrics on a per-node basis. Other studies, such as [12], compared multiple routing protocols in NS-2, while [13] focused on IEEE 802.11p in a V2X (Vehicle-to-Everything) context without comparing it against LPWAN (Low-Power Wide-Area Network) approaches.

While these studies provide valuable insights at the protocol level, they fail to explore hybrid integration of V2X and LPWAN technologies. Additionally, they do not conduct systematic cross-technology comparisons under consistent physical and mobility conditions.

B. LoRaWAN Studies in Mobile Context

Most research on LoRaWAN has focused on static or low-mobility deployments, emphasizing scalability, interference management, and the efficiency of the ADR mechanism. Authors in [1] simulated LoRaWAN [5]-Aloha and LoRaWAN-CSMA/CA in NS-3 [8], but without realistic mobility traces or detailed PHY/MAC instrumentation. Authors in [3] proposed a distance-based geographic allocation strategy for the Spreading Factor (SF), yet without synchronization to transmission cycles or consideration of mobility dynamics.

A few studies have attempted to assess LoRaWAN under mobility like in [6]n where authors combined real-world RSSI measurements and NS-3 [8] simulations to evaluate different mobility models (Random Waypoint, Gauss-Markov), but using only a limited number of vehicles. Also, authors in [4] proposed cross-validation between field experiments and simulations but relied on just two vehicles—insufficient to characterize LoRaWAN behavior under dense mobility. Similarly, authors in [7] demonstrated the feasibility of LoRa in urban vehicular contexts, yet without accounting for complex radio environments or realistic topologies.

More recent efforts, such as in [14], where authors examined continuous mobility scenarios and highlighted the influence of speed and obstacles on PDR. However, these studies did not consider dense urban topologies or multi-vehicle conditions. Other works, such as in [15] and [16], explored the impact of physical parameters (SF, CR, TX power) and gateway optimization strategies, but without incorporating mobility or temporal instrumentation.

These prior approaches share several key limitations:

- Absence of realistic urban topologies (buildings, tunnels, and complex roads);
- Limited or no SUMO/OSM-based mobility traces;
- Lack of temporal PHY/MAC instrumentation (SNR, RSSI, collisions, latency, jitter);
- No open datasets or reproducible simulation frameworks available to the community.

C. Identified Gaps and Positioning of the Present Work

To date, no prior work has conducted a direct comparative evaluation between LoRaWAN and IEEE 802.11p under identical V2I conditions, ensuring:

- Identical physical and urban geometry (buildings, tunnels, roads),
- Consistent SUMO [9]-based mobility traces,
- Equivalent traffic scheduling and evaluation metrics,
- Frequency-calibrated propagation models.

Furthermore, no existing simulation framework enables fine-grained instrumentation and reproducible cross-technology analysis between these two paradigms. This paper therefore introduces the first unified simulation framework addressing this gap.

III. Simulation Environment and Methodology

A. Simulation Architecture

To ensure a fair and reproducible comparison between LoRaWAN and IEEE 802.11p, and to assess the feasibility of LoRa-based communication in vehicular environments, it was essential to rely on a robust and validated LoRaWAN module for NS-3. This is why we choose the module presented in citeref5, which is currently the most widely adopted implementation within the NS-3 research community. However,

this module was originally designed for static IoT deployments and does not natively support vehicular mobility. To overcome these limitations and enable the LoRaWAN module [5] to operate in a VANET environment, we have introduced several functional extensions:

- Dynamic mobility integration with real-time updates of LoRaWAN [5] nodes;
- Adaptive link evaluation;
- Extended physical layer with incorporation of Doppler shift effects.

This architecture ensures that the observed performance differences between the two technologies are solely attributable to their underlying radio and propagation mechanisms.

The seamless integration of OSM, SUMO [1], and NS-3 [8] provides both high realism and full reproducibility—two essential requirements for experimental studies targeting next-generation vehicular networks.

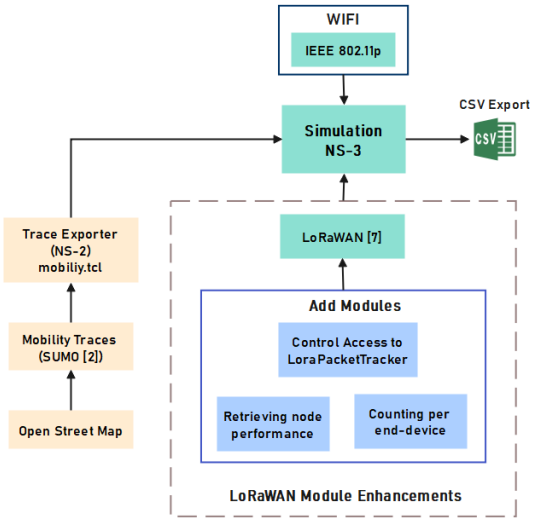

Fig. 1: Overall simulation architecture for LoRaWAN and IEEE 802.11p environment in NS-3

B. Common Physical Environment

The simulated environment replicates a real mixed urban-peri-urban corridor (Colmar, France), including buildings, tunnels, dense intersections, and open road segments. Radio conditions were modeled using the HybridBuildingsPropagationLossModel, which incorporates:

- Free-space attenuation as a function of distance,
- Wall penetration and diffraction effects,
- Multipath reflection from surrounding structures,
- Log-normal shadowing $X_\sigma \sim \mathcal{N}(0, \sigma^2)$.

The total path loss is expressed as:

$$L_{\text{tot}}(d) = L_{\text{path}}(d) + L_{\text{wall}} + L_{\text{height}} + X_\sigma, \tag{1}$$

where L_{path} depends on the visibility condition (LOS/NLOS).

This choice is particularly relevant for vehicular communications, where short-term topological variations—such as entering a tunnel or passing behind obstacles—strongly affect link stability and radio connectivity duration. Antenna heights were fixed at 1.5 m for vehicles and 15 m for RSUs/gateways, consistent with ITS-G5 and LoRa Alliance deployment standards. This ensures that performance variations stem solely from radio physics (frequency, attenuation, diffraction), not from geometric bias. The hybrid model captures fast transitions between LOS and NLOS states, characteristic of dynamic vehicular environments, while balancing realism and computational efficiency.

C. Frequency and Propagation Models

Each technology was associated with a propagation model calibrated to its operational frequency band to ensure physical validity and comparability of results.

1) LoRaWAN (868 MHz): employs the HybridBuildingsPropagationLossModel combined with log-normal shadowing ($\sigma = 6$ dB) and a Nakagami-m fading process. The path loss is expressed as:

$$PL(d) = PL_0 + 10\eta \log_{10}(d) + X_\sigma, \tag{2}$$

with $PL_0 = 46.68$ dB and $\eta = 2.7$.

The received power is given by:

$$P_{Rx} = P_{Tx} - PL(d) - S, \tag{3}$$

where S denotes instantaneous fading. The symbol time is defined as: $T_s = \frac{2^{SF}}{BW}$, and the total ToA as:

$$T_{ToA} = (T_{\text{preamble}} + T_{\text{payload}}) \tag{4}$$

The sub-GHz band provides strong diffraction and penetration capabilities, offering enhanced robustness at long range and under NLOS conditions. This parameterization aligns with empirical LPWAN measurements and accurately represents LoRaWAN behavior in mobile urban scenarios.

2) IEEE 802.11p (5.9 GHz): was modeled using the ThreeGppV2vPropagationLossModel, configured for both *Urban Macro (UMa)* and *Highway* scenarios, as defined in 3GPP TR 37.885. The probability of line-of-sight is given by:

$$P_{LoS}(d) = \min(1.0,\, 1.05e^{-0.0114d}), \tag{5}$$

and the corresponding path losses are:

$$L_{LoS}(d) = 38.77 + 16.7\log_{10}(d) + 18.2\log_{10}\left(\frac{f}{1\,\text{GHz}}\right), \tag{6}$$

$$L_{NLoS}(d) = 36.85 + 30\log_{10}(d) + 18.9\log_{10}\left(\frac{f}{1\,\text{GHz}}\right). \tag{7}$$

A Gaussian shadowing ($\sigma = 4$ dB) and a Jakes fading model were applied to account for small-scale fading and Doppler spread, where the Doppler frequency is:

$$f_D = \frac{v f_c}{c}. \tag{8}$$

This model captures the characteristic behavior of the 5.9 GHz band—short range, high throughput, and low latency—contrasting with the long-range but delay-tolerant nature of LoRaWAN.

D. Reproducibility and Instrumentation

Scientific reproducibility was central to the methodology. Both simulation frameworks share a unified instrumentation pipeline based on automatic CSV exports, extending *LoraPacketTracker* and *WifiStatsHelper* files to capture fine-grained temporal and spatial statistics at per-node and per-packet granularity. The collected performance metrics include:

- PDR: measures the reliability of packet transmissions between nodes.
- Latency: quantifies the average end-to-end transmission delay.
- Effective Throughput: represents the average useful data successfully received per unit of time.

All metrics were extracted and processed using identical data pipelines across both LoRaWAN [5] and IEEE 802.11p scenarios to ensure comparability and experimental fairness.

Simulation outputs were exported as structured datasets to foster reproducibility and enable future research on AI-based parameter optimization and cross-technology predictive modeling. This methodology—rooted in experimental rigor, transparency, and reproducibility—fully aligns with the research ethics and scientific standards upheld by the community scientific.

IV. Results, Analysis and Discussions

A. Experimental Parameters

To ensure a fair and reproducible comparison between the two technologies, all simulations were executed in NS-3 using the extended LoRaWAN module [5] and the native *WAVE* stack. The experiments follow a pure V2I configuration, where vehicular nodes communicate periodically with fixed gateways or RSUs, isolating PHY/MAC effects from application-layer interference. Table I summarizes the main parameters used throughout the simulations.

TABLE I: Simulation parameters for the two technologies.

Parameter	LoRaWAN	IEEE 802.11p
Simulation area (R)	500 m–8 km^2	500 m–8 km^2
Number of vehicles (V)	50–200	50–200
Number of GW/RSU	4	4
Payload	12 B every 60 s	12 B every 60 s
Transmission power	+14 dBm	+23 dBm
Antenna gain	-	3 dBi
Antenna height (vehicles / RSUs)	1.5 m / 15 m	1.5 m / 15 m
Propagation model	HybridBuildings Loss+Nakagami	3GPP V2V Urban + Jakes
Shadowing variance (σ)	6 dB	4 dB
Bandwidth	125 kHz	10 MHz
Carrier frequency	868 MHz	5.9 GHz
Simulation duration	3600 s	3600 s
Mobility source	SUMO traces (OSM)	SUMO traces (OSM)

This configuration ensures methodological alignment between frequency band, propagation model, and mobility dynamics. The adoption of standardized antenna gains and heights eliminates geometric bias, while the use of periodic low-rate UDP traffic isolates radio-layer performance. Such consistency guarantees that the observed differences in PDR, latency, and throughput arise purely from the intrinsic characteristics of each technology.

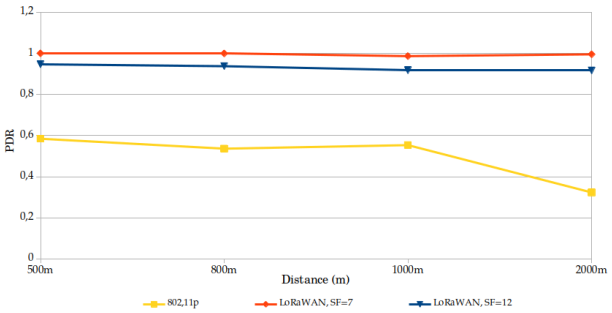

Fig. 2: PDR vs Network radius - V=50

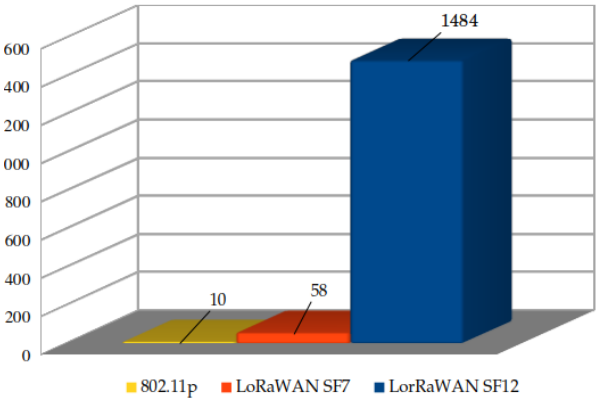

Fig. 3: Average latency comparison - V=50 - R=1 km

B. Comparative Evaluation: IEEE 802.11p vs LoRaWAN

We begin our evaluation by comparing the reliability of IEEE 802.11p and LoRaWAN as the network radius varies. We notice that for simplicity reason, we only use SF7 and SF12 to compare with the IEEE 802.11p. As depicted in Fig. 2, the LoRaWAN solution maintains a PDR above 90% even at 2 km, whereas IEEE 802.11p drops below 50% at just 800 m. This discrepancy arises from the 5.9 GHz propagation model, which exhibits higher attenuation and lower diffraction. In contrast, LoRaWAN's sub-GHz band offers superior resilience to obstruction-induced losses. The use of the *ThreeGppV2vUrbanPropagationLossModel* for IEEE 802.11p accurately reproduces these effects, consistent with UMa/NLOS profiles defined in 3GPP TR 36.885.

Concerning the obtained latency, Fig 3 reveals a clear contrast: IEEE 802.11p achieves nearly 10 ms, LoRa SF7 achieves 58 ms, and LoRa SF12 achieves nearly 1.48 s. This confirms the fundamental design dichotomy between the two technologies:

- IEEE 802.11p: designed for instantaneous, short-range, reactive communication (V2V/V2I safety messages).
- LoRaWAN: optimized for long-range, low-power, and delay-tolerant IoT connectivity.

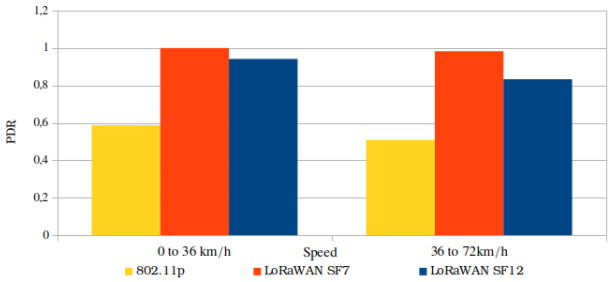

Fig. 4: Mobility impact on PDR - V=50 - R=800 m

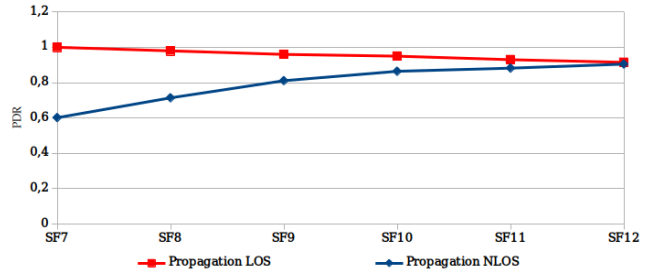

Fig. 5: PDR vs SF: comparison between *non-obstructed* and *obstructed* scenario - V=100 - R=3 km

The measured values are consistent with previous experimental studies (e.g., ETSI EN 302 663, LoRa Alliance TechSpec v1.0.4), confirming the validity and accuracy of the simulation framework.

To continue our evaluation, we vary the vehicles' velocities. The Fig. 4) demonstrates that LoRaWAN reliability remains nearly constant between 0 and 72 km/h, while IEEE 802.11p shows a sharp decline due to Doppler-induced variability and frequent link disruptions. LoRaWAN's stability is attributed to its long symbol duration, which mitigates the effects of fast channel variations and makes the PHY layer more resilient to vehicular mobility.

Overall, the results underline the complementary nature of both technologies:

- IEEE 802.11p excels in low-latency, short-range, safety-critical applications requiring fast message exchange (e.g., collision avoidance).
- LoRaWAN, by contrast, provides a robust long-range and energy-efficient alternative suitable for telemetry, environmental monitoring, and V2I data aggregation.

These findings justify the interest of LoRaWAN as a potential communication technology for V2X architectures, where it can offload non-critical traffic, extend coverage, and ensure persistent connectivity in areas where high-frequency links are unreliable.

C. LoRaWAN Behavior in VANET Context

To study the impact of the environment (buildings, obstacles, etc.) on the reliability, we compare a LOS scenario against an NLOS one, where both scenarios experience the same number of vehicles and the same simulation area (3 km). As shown in Fig. 5, in the non-obstructed environment, the PDR slightly decreases with increasing SF, from 100% at SF7 to approximately 90% at SF12. This behavior results from the longer transmission time and the higher probability of packet collisions associated with larger SFs under favorable radio conditions [2]. Conversely, in the obstructed scenario, the PDR increases with the SF, rising from 60% at SF7 to 88% at SF12, since higher SFs provide greater receiver sensitivity and stronger resilience to noise, multipath fading, and non-line-of-sight propagation. These results clearly demonstrate that higher SFs are less affected by obstructions, whereas lower SFs exhibit pronounced degradation in complex urban environments.

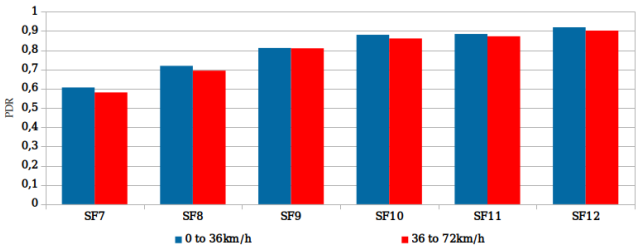

Fig. 7: Mobility and SF impact on PDR - V=100 - R=3 km

In the remaining discussion, we show only the results of obstructed scenarios (NLOS).

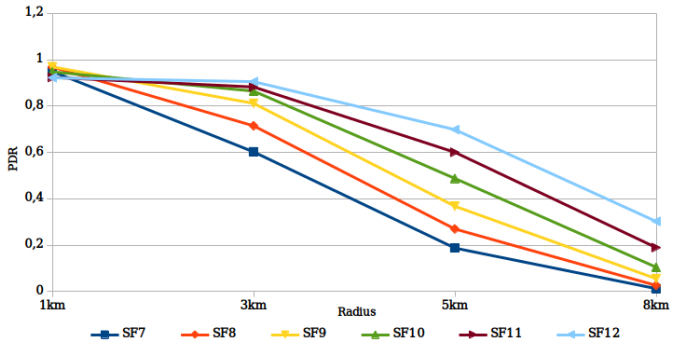

Fig. 6: PDR vs Network radius - V=100

Fig. 6 shows that the PDR decreases progressively as the communication distance increases for all SF. At 1 km, all configurations achieve a PDR above 90%, indicating stable propagation with negligible packet losses. At 3 km, the performance begins to diverge: SF7 drops to around 65%, while SF12 still maintains nearly 90%, highlighting its higher resilience to attenuation. When the distance reaches 5 km, degradation becomes more pronounced—SF7 falls below 20%, whereas SF11 and SF12 remain around 60% and 70%, respectively. At the maximum observed range (8 km), only SF12 sustains a PDR above 30%, while all other SF drop below 20%, rendering them ineffective for long-range communication. These results confirm that higher SF ensure greater link reliability over extended distances, whereas lower SFs exhibit a sharp decline in performance due to increased path loss and reduced signal-to-noise ratio with distance.

Fig. 7 shows how mobility slightly reduces the PDR across

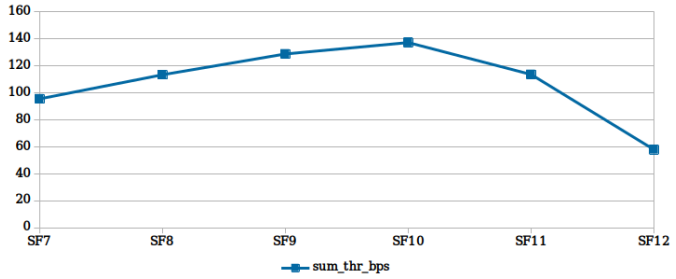

Fig. 8: Aggregated throughput (bps) vs SF - V=100 - R=3 km

all SF values, with a more pronounced impact on SF7–SF9. At higher speeds, the channel experiences increased Doppler shifts and more frequent transitions; short-symbol SFs, having lower sensitivity, are more vulnerable to synchronization and demodulation errors. Conversely, higher SFs mitigate these variations thanks to their longer symbol durations, which smooth out rapid channel fluctuations—hence their relative stability in dynamic vehicular environments.

Fig. 8 illustrates the variation of the aggregated throughput as a function of the SF in a dense urban LoRaWAN-VANET scenario. Overall, the results show that system performance improves progressively from SF7 to SF10, with the throughput reaching its maximum (approximately 140 bps). Beyond this point, a noticeable decline is observed as the SF increases to SF11 and SF12. This trend highlights a trade-off inherent to LoRa modulation: higher SF values enhance signal robustness and transmission range but simultaneously increase the ToA, leading to longer channel occupancy and reduced network capacity. Conversely, smaller SFs provide higher bitrates but are more susceptible to packet loss and collisions due to limited coverage.

Consequently, SF10 emerges as an optimal configuration for this urban vehicular scenario, offering a balanced compromise between coverage reliability and spectral efficiency. The results also confirm that excessive spreading (SF11–SF12) significantly degrades the overall network throughput due to prolonged transmission times and increased medium contention.

V. Conclusion

This paper presented a reproducible comparative evaluation of LoRaWAN and IEEE 802.11p for V2I communications using a unified NS-3 framework integrated with SUMO mobility and a HybridBuildings propagation model. Results show that LoRaWAN achieves up to 90% reliability at 2 km with moderate latency (0.5–1.5 s), while IEEE 802.11p maintains sub-10 ms delay within 1 km but rapidly degrades under NLOS conditions. These findings highlight the complementary strengths of both technologies: LoRaWAN provides large-scale, delay-tolerant coverage, whereas IEEE 802.11p ensures low-latency responsiveness for safety-critical applications. This work demonstrates that combining LPWAN and DSRC technologies can bridge the connectivity gap between dense urban and wide-area vehicular environments. The proposed framework and released open dataset establish a reproducible foundation for future research on hybrid LoRaWAN–802.11p architectures, where AI-driven adaptive PHY mechanisms could dynamically optimize the trade-off between latency, coverage, and reliability under vehicular mobility.

References

[1] A. Farhad, G.-R. Kwon, and J.-Y. Pyun, "Mobility adaptive data rate based on kalman filter for lora-empowered iot applications," in *2023 IEEE 20th Consumer Communications Networking Conference (CCNC)*, 2023, pp. 321–324.

[2] M. C. Bor, U. Roedig, T. Voigt, and J. M. Alonso, "Do lora low-power wide-area networks scale?" in *Proceedings of the 19th ACM International Conference on Modeling, Analysis and Simulation of Wireless and Mobile Systems*, ser. MSWiM '16. New York, NY, USA: Association for Computing Machinery, 2016, p. 59–67. [Online]. Available: https://doi.org/10.1145/2988287.2989163

[3] T. Yatagan and S. Oktug, "Smart spreading factor assignment for lorawans," in *2019 IEEE Symposium on Computers and Communications (ISCC)*, 2019, pp. 1–7.

[4] F. M. Ortiz, T. T. de Almeida, A. E. Ferreira, and L. H. M.K. Costa, "Experimental vs. simulation analysis of lora for vehicular communications," *Computer Communications*, vol. 160, pp. 299–310, 2020. [Online]. Available: https://www.sciencedirect.com/science/article/pii/S0140366419319966

[5] D. Magrin, M. Capuzzo, S. Romagnolo, and M. Luvisotto, "An ns-3 module for the simulation of lorawan networks," https://github.com/signetlabdei/lorawan, 2019, accessed: 2025-05-01.

[6] N. Abdelouahab, T. A. Mounir, and S. Boumerdassi, "Impact of mobility model on lorawan performance," *Journal of Communications*, vol. 19, pp. 7–18, 01 2024.

[7] T. Karunathilake and A. Förster, "Using lora communication for urban vanets: Feasibility and challenges," 2023. [Online]. Available: https://arxiv.org/abs/2311.18070

[8] ns-3 Consortium, "ns-3.45: Network Simulator 3," https://www.nsnam.org/releases/ns-3-45/, Jun. 2025, released June 1, 2025. Includes new DHCPv6 model, 320 MHz Wi-Fi support, EMLSR improvements, and other maintenance updates.

[9] D. Krajzewicz, J. Erdmann, M. Behrisch, and L. Bieker-Walz, "SUMO 1.24.0: Simulation of Urban Mobility," https://sumo.dlr.de/docs/, August 2024, open-source traffic simulation suite developed by the DLR Institute of Transportation Systems.

[10] K. N. Tayade and M. U. Kharat, "Mobility prediction and enhancement of link stability in VANET using MGPSR and MAODV protocol," *International Journal of Engineering Trends and Technology*, vol. 70, no. 3, pp. 66–74, 2022. [Online]. Available: https://doi.org/10.14445/22315381/IJETT-V70I2P208

[11] E. Spaho, A. Biberaj, and A. Tahiraga, "Lorawan for an iot-based environmental monitoring application in tirana city," *Pollack Periodica*, vol. 16, no. 2, pp. 92 – 97, 2021. [Online]. Available: https://akjournals.com/view/journals/606/16/2/article-p92.xml

[12] G. Singh, M. Prateek, S. Kumar, M. Verma, D. Singh, and H.-N. Lee, "Hybrid genetic firefly algorithm-based routing protocol for vanets," *IEEE Access*, vol. PP, pp. 1–1, 01 2022.

[13] A. Sassi, Y. Elhillali, and F. Charfi, "Evaluating experimental measurements of the ieee 802.11p communication using arada locomate obu device compared to the theoretical simulation results," *Wireless Personal Communications*, vol. 97, no. 3, pp. 3861–3874, Dec 2017. [Online]. Available: https://doi.org/10.1007/s11277-017-4703-4

[14] L. C. da Rocha Santos, S. M. Bruschi, P. S. L. de Souza, J. Ueyama, A. de Jesus dos Santos, and J. S. Barbosa, "Performance analysis of a vehicular ad hoc network using lora technology and iot devices in amazon rivers," *Ad Hoc Networks*, vol. 152, p. 103301, 2024. [Online]. Available: https://www.sciencedirect.com/science/article/pii/S1570870523002214

[15] J. Spišić, A. Pejković, M. Zrnić, V. Križanović, K. Grgić, and D. Žagar, "Lorawan parameters optimization for efficient communication," in *2022 International Conference on Smart Systems and Technologies (SST)*, 2022, pp. 335–339.

[16] B. Yu, Y. Bao, Y. Huang, W. Zhan, and P. Liu, "Modeling and throughput optimization of multi-gateway lorawan," *IEEE Access*, vol. 11, pp. 142 940–142 950, 2023.